Engineering of peptide b-sheet nanotapes†

Amalia Aggeli, Mark Bell, Neville Boden,* Jeff N. Keen, Tom C. B. McLeish, Irina Nyrkova, Sheena E. Radford and Alexander Semenov

Centre for Self Organising Molecular Systems, School of Chemistry, The University of Leeds, Leeds, UK LS2 9JT

A set of principles are outlined for the design of short oligopeptides which will self-assemble in appropriate solvents into long, semi-flexible, polymeric b-sheet nanotapes. Their validity is demonstrated by experimental studies of an 11-residue peptide (DN1) which forms nanotapes in water, and a 24-residue peptide (K24) which forms nanotapes in non-aqueous solvents such as methanol. Circular dichroism (CD) spectroscopy studies of the self-assembly behaviour in very dilute solutions (mM) reveal a simple transition from a random coil-to-b-sheet conformation in the case of DN1, but a more complex situation for K24. Association of DN1 is very weak up to a concentration of 40 mM at which there is a sudden increase in the fraction of peptide in the b-sheet structure, indicative of an apparent 'critical tape concentration'. This is shown to arise from a two-step self-assembly process: the first step being a transition from a random coil to an extended b-strand conformation, and the second the addition of this b-strand to a growing b-sheet. Both peptides are shown to gel their solvents at concentrations above 2×10^{-3} volume fraction: these gels are stable up to the boiling point of the solvents. Rheology measurements on gels of the 24-residue peptide in 2-chloroethanol reveal that the tapes form an entangled network with a mesh size of 10–100 nm for peptide volume fractions 0.03–0.003; the persistence length of the tape is 13 nm or greater, indicative of a moderately rigid polymer; the tapes are about a single molecule in thickness. The mechanical properties of the gels in many respects are comparable to those of natural biopolymers such as gelatin, actin, amylose and agarose.

Self-assembly of complementary molecular components through hydrogen bonding is emerging as a novel synthetic route to linear polymeric structures. Polymer tapes have been synthesised[1–3] from nucleoside-like components (triaminopyrimidines/triazine barbiturates) and shown to form gels in certain organic solvents.[4] These are essentially self-assembling ladder polymers.[5] Biaxial polymers are of special interest, since they are expected to have quite different physics from classical, uniaxial linear polymers.[6] Whilst the polymer will bend freely in one plane, it will be relatively rigid in the perpendicular direction. However, at long enough length scales, out of plane fluctuations are expected to lead to disc-like objects and, at even longer length scales, to three-dimensional coils. Consequently, solutions of tape-like polymers are predicted to form mesophases at high enough concentrations. Self-assembling tape-like polymers can be expected, therefore, to exhibit far more complex behaviour.

We have been exploring an alternative generic route to tape-like polymers. This exploits the propensity of peptide chains to self-assemble *via* intermolecular or intramolecular hydrogen bonding into b-sheet structures. Such structures exist widely as short b-sheets or barrels in proteins, and also as extended b-sheets in silk.[7]

Here, we demonstrate that oligopeptides of minimal complexity, can be designed to self-assemble in solution to form long, semi-flexible, polymeric b-sheet tapes, a single molecule in thickness. At volume fraction concentrations 0.001–0.005, the tapes become entangled to form gels with viscoelastic properties in some ways analogous to, but in other ways distinct from, those observed for gels of classical synthetic polymers. The shape and dimensions of the polymers are established by transmission electron microscopy, the conformation of the peptides and their self-assembly (secondary and tertiary structures) are monitored in dilute solutions by circular dichroism spectropolarimetry, and in semi-dilute solutions by FTIR spectroscopy, whilst information about the properties of the networks in the gels formed at higher concentrations is obtained by rheological measurements.

Peptide Design

The objective is to design a peptide of minimal complexity, which will self-assemble into elongated, antiparallel b-sheet tapes in a particular solvent. This requires a large negative free energy change for the transformation of a monomeric helical/random coil peptide from solution to the end of a growing tape (Scheme 1).

It is believed that a peptide must have a minimum of six residues to form stable b-sheet structures.[8,9] The relative stability of a b-sheet as compared to helix or random coil is believed to stem, not from the differences in hydrogen bonding energies, but rather from the forces between the side-chains of neighbouring amino acids and the solvation energies of these side-chains. These interactions must be sufficient to fully compensate for the loss of translational and conformational entropies of the peptide molecule as it is 'frozen' into the relatively rigid b-sheet organisation. It is also essential to incorporate an element of molecular recognition into the side-chain interactions. This is to ensure that the peptides arrange themselves into the requisite antiparallel tape-like structures in preference to an interdigitated two-dimensional b-sheet. It is also essential that the medium acts as a good solvent for the polymer tape.

These considerations lead us to the following working criteria for the rational design of peptides to produce b-sheet tapes in solution: (*i*) cross-strand attractive forces (hydrophobic, electrostatic, hydrogen-bonding) between side-chains, (*ii*) lateral recognition between adjacent b-strands to constrain their self-assembly to one dimension, and avoid heterogeneous aggregated b-sheet structures, and (*iii*) strong adhesion of solvent to the surface of the tapes to control solubility.

The work presented in this paper focuses on the behaviour of two distinctly different peptides K24 and DN1, which have been designed to self-assemble into b-sheet tapes in, respectively, moderately polar (non-aqueous) and highly polar (aqueous) media.

† A preliminary account of this work has been published in *Nature*, 1997, **386**, 259.

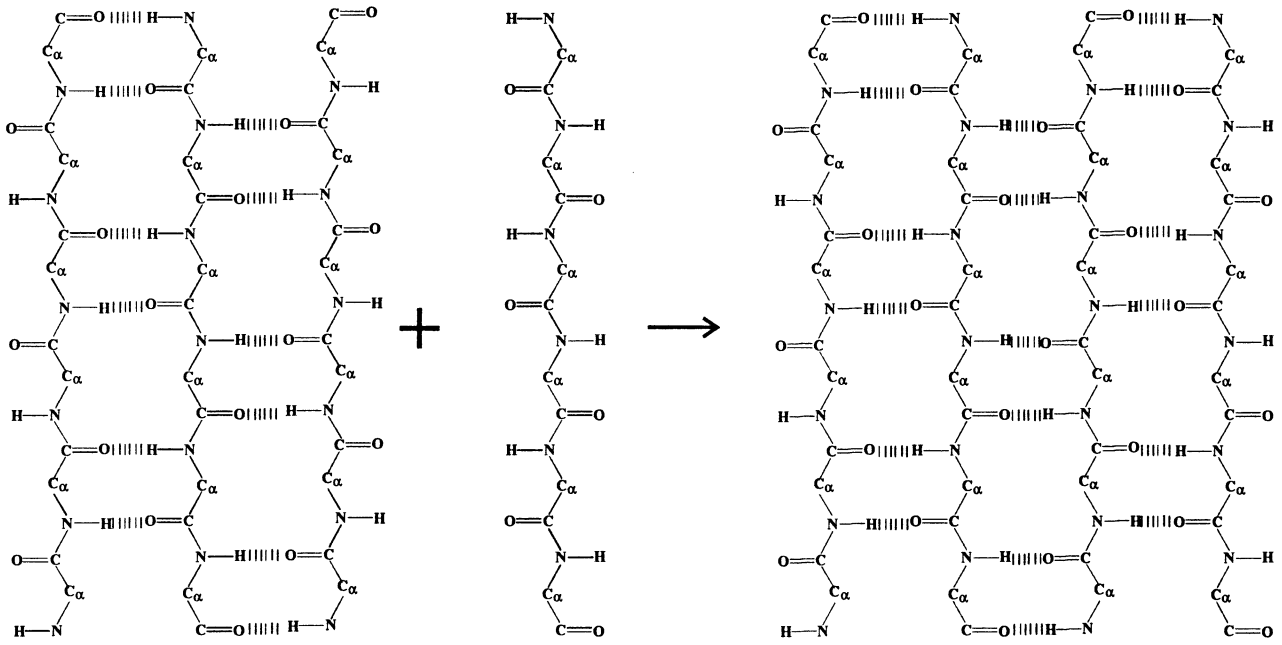

Scheme 1 Schematic representation of the self-assembly of six-residue peptide molecules to form a growing intermolecular antiparallel b-sheet tape. Hydrogen bonding between backbones of adjacent peptide b-strands is indicated.

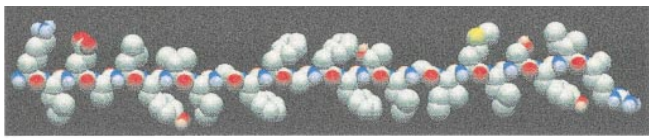

(*a*)

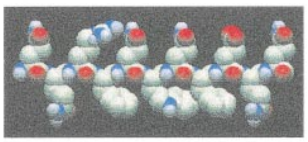

(*b*)

Fig. 1 Space-filling models of (*a*) K24 and (*b*) DN1 peptides in an extended b-strand conformation. Colour code: white = hydrogen, red = oxygen, blue = nitrogen, yellow = sulfur, black = carbon.

The primary structure of the 24-residue peptide K24, NH_2-Lys-Leu-Glu-Ala-Leu-Tyr-Val-Leu-Gly-Phe-Phe-Gly-Phe-Phe-Thr-Leu-Gly-Ile-Met-Leu-Ser-Tyr-Ile-Arg-COOH, [Fig. 1(*a*)] is related to the single transmembrane domain of the IsK protein.[10] Its longer 27-residue version, K27, is known to readily form b-sheet structures in lipid bilayers,[11] suggesting these peptides would be good candidates for formation of b-sheet tapes in amphiphilic solvents such as methanol and 2-chloroethanol. Furthermore, the amphiphilicity along the K24 molecule (polar side-chains predominantly near the peptide termini, and apolar side-chains predominantly in the middle of the peptide chain) is expected to favour the alignment of the peptide b-strands with respect to each other, which will lead to the one-dimensional propagation of the b-sheet. Such an intermolecular arrangement would thus allow the establishment of several kinds of favourable contacts along adjacent peptide b-strands: for example, intermolecular interactions between polar side-chains (such as Lys1, Glu3 and Arg24) near the termini, between non-polar side-chains (such as Leu5, Val7, Leu8, Leu16, Ile18 and Leu20) in the central region of the peptide chain, as well as specific interactions such as p–p interactions among the four aromatic phenylalanine rings at positions 10, 11, 13 and 14.

The design of the 11-residue peptide DN1, CH_3CO-Gln-Gln-Arg-Phe-Gln-Trp-Gln-Phe-Glu-Gln-Gln-NH_2 [Fig. 1(*b*)], is not based on any native protein. Rather it has been rationally designed to form b-sheet polymer tapes in water. The $(-CH_2-)_2$ moieties of the six glutamine residues are expected to provide attractive intermolecular hydrophobic interactions between side-chains. The residues Phe4, Trp6 and Phe8 are also hydrophobic, but they are also expected to provide intermolecular recognition by p–p interactions.[12,13] Arg3 and Glu9 provide an additional degree of recognition *via* their strong coulombic attraction,[12] and favour an antiparallel alignment of the strands. Gln, Arg and Glu side-chains make one surface of the b-sheet more hydrophilic than the other. Chemically blocked termini were used to avoid edge-to-edge coulombic attractions between tapes.

Materials and Experimental Methods

Peptide synthesis

Standard automated solid phase methods were employed for the synthesis of the peptides. The synthesis of K24 was carried out as described in ref. 11 for K27. Solid-phase synthesis of peptide DN1 was also performed using Fmoc-chemistry (Fmoc: fluoren-9-ylmethoxycarbonyl). The peptide was assembled on PEG–PS (polyethylene glycol–polystyrene) resin, incorporating a linker to generate the C-terminal amide upon cleavage of the peptide from the resin. Fmoc-amino acids were C-terminally activated using Hbtu [2-(1*H*-benzotriazol-l-yl)-1,1,3,3-tetramethyluronium hexafluorophosphate] with DIPEA (diisopropylethylamine). The resin-bound peptide was *N*-terminally acetylated by reaction with 0.3 M acetic anhydride–0.03 M pyridine in DMF (dimethylformamide) (10 min at room temp.). Cleavage of the peptide from the resin and deprotection of amino acid side-chains were achieved by incubation for 1 h in TFA (trifluoroacetic acid), containing 1% (w/v) phenol, 2% (v/v) water, 4% (v/v) ethane-1,2-dithiol and 2% (v/v) anisole. The peptide was precipitated with diethyl ether, centrifuged and washed a further 4 times with diethyl ether. The diethyl ether was evaporated and the peptide dissolved in water for purification by reversed-phase HPLC, which was carried out using water–acetonitrile gradient in the presence of 0.1% TFA. Mass spectrometry has shown that the

molecular masses are as expected (K24: m/z 2800 and DN1: m/z 1593). K24 was shown by ^{19}F NMR and FTIR to contain *ca.* 4 mols of residual TFA per 1 mol peptide. Less TFA (*ca.* 2 mol TFA/mol peptide) is present in DN1, on the basis of FTIR. Peptides were stored in their lyophilised state. The gelation properties and self-assembly behaviour of 0.007 v/v K24 solutions as monitored by FTIR are independent of the method used to prepare the samples, *i.e.* starting from either a predominantly helical or a mixture of helical–b-sheet conformations in the original lyophilised sample.

Experimental techniques

FTIR spectroscopy. Spectra were averages of four scans, recorded with a resolution of 4 cm^{-1}, at 20 °C in an FTIR liquid cell equipped with CaF_2 crystals and a 50 mm Teflon spacer, using a Perkin-Elmer 1760X FTIR spectrometer. After subtraction of the solvent spectrum, the component peaks of the peptide amide I band were obtained by second derivative analysis and peak-fitting of the absorption spectra, using a home-written program, consisting of iterative adjustment of the relative heights, widths and ratios of Lorenzian–Gaussian functions of the lineshapes of the individual components, to obtain the best fit between the spectrum calculated by the program and the experimental one.

CD spectroscopy. Measurements were obtained with a Jasco J-715 spectropolarimeter using 1 mm and 1 cm quartz cuvettes at 20 °C. Spectra were recorded with a step resolution of 1 nm, a scan speed of 50 nm min^{-1}, a sensitivity of 50 millidegrees and a response time of 1 s. Each spectrum was the average of 4–10 scans. The peptide concentration in solution was determined by amino acid analysis and ninhydrin assay.

Transmission electron microscopy (TEM). Fig. 2(*a*) was obtained using a 0.001 v/v (500 mM) K24 gel in methanol after dilution to 25 mM peptide concentration. The copper EM grids were of mesh size 300 (corresponding to grids with 300 bars per inch) and were coated with carbon films. The carbon films were glow-discharged in order to build static charges. A droplet of the peptide solution was deposited on a clean surface. Each grid was then deposited on top of the sample droplet for 1 min, so that the peptide network was adsorbed onto the surface of the carbon film. Excess sample was drained off the grid. The grid was then introduced on top of a droplet of uranyl acetate (UA) negative staining solution in water (4 g UA per 100 ml water) for 20 s and excess of the staining solution was drained off the grid. Fig. 2(*c*) was obtained with a starting solution of 0.001 v/v (500 mM) K24 in deionised water. The opalescent solution was centrifuged to remove the largest particles. A droplet of the supernatant was used to prepare a grid in the same way as above. The specimens were allowed to air-dry. Fig. 2(*a*) was obtained with a Phillips CM10 TEM at 100 kV accelerating voltage, set at 105 000 ± 5% magnification, whilst Fig. 2(*b*) and (*c*) were obtained with a Jeol 100S TEM operating at 100 kV and set at 50 000 ± 5% magnification. The pictures were enlarged during printing to attain the total sample magnification which appears in the individual figure legends. Care was taken to obtain a photographic record of the specimens as quickly as possible after sample insertion, in order to minimise artefacts which can be caused by long exposure of the sample to high vacuum and the intense electron beam.

Rheology. A Rheometrics Dynamic Analyser II, with 25 mm diameter parallel plate geometry, was employed. The thickness of the material between the plates was between 0.5 and 0.8 mm. Gels were prepared 3 d prior to the measurements. The following precautions were taken to minimise the problem of solvent evaporation from the periphery of the sample between the two parallel plates. First, most gels were prepared in 2-chloroethanol. Its high boiling point compared to the other gel-favouring solvents minimises the solvent evaporation rate and changes of peptide concentration. Secondly, the oven, which surrounds the sample, was kept closed during data collection. Thirdly, two containers full of solvent were kept near the

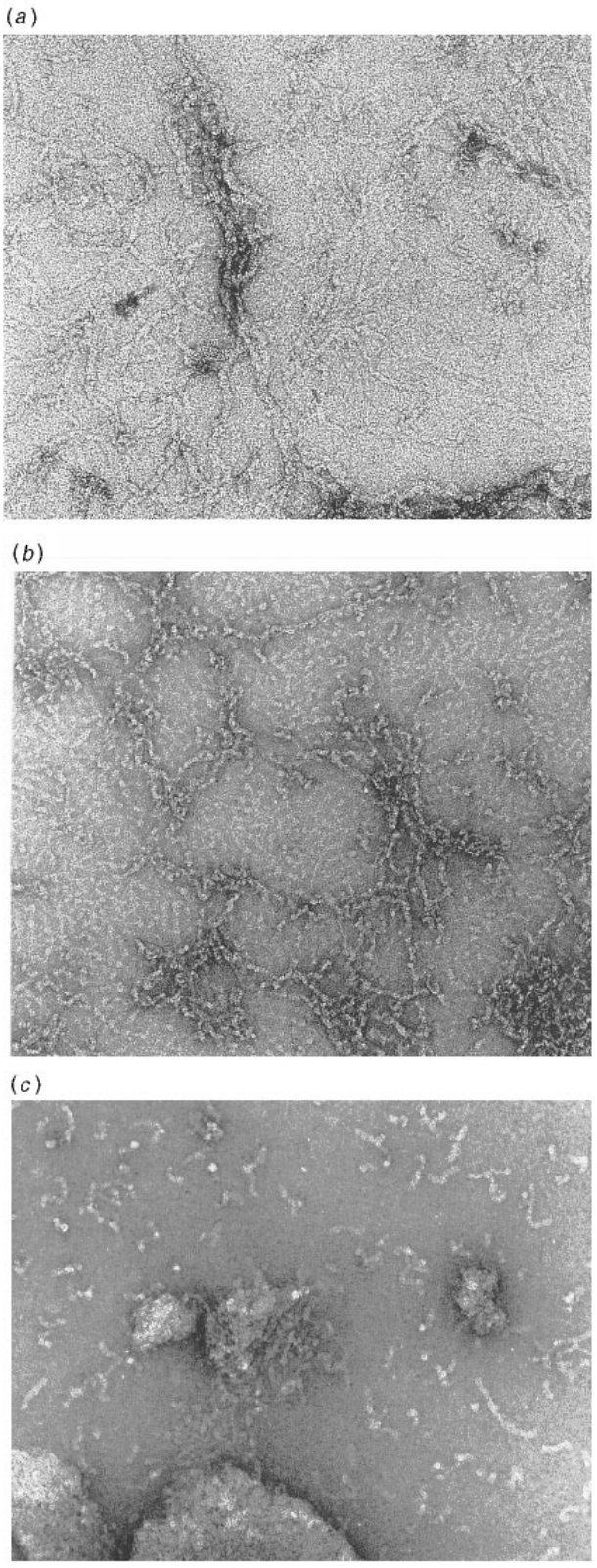

Fig. 2 TEM micrographs of b-sheet structures of K24 stained with uranyl acetate and adsorbed on carbon-coated, glow-discharged grids: (*a*) network of a 0.001 v/v (500 mM) K24 gel in methanol, following twentyfold dilution; (*b*) network of a 0.001 v/v K24 gel in methanol, without prior dilution; (*c*) insoluble peptide in water. Total magnification: × 262 000.

sample, inside the oven, to saturate the atmosphere with solvent vapour. Furthermore, the air flow system (which is used to control sample temperature) was turned off, and the experiments were carried out at ambient temperature. Temperature fluctuations of the sample were closely monitored.

Results

General observations

When K24 is added to solvents such as ethanol, methanol or 2-chloroethanol, at a peptide volume fraction of *ca.* 0.002 v/v (*ca.* 3 mg ml^{-1}), the dry peptide particles initially swell, and eventually coalesce to form a transparent, homogeneous gel. This procedure takes place over several hours depending on peptide concentration, solvent and temperature. The gels are stable for months at room temperature. They are optically isotropic, but become optically birefringent when sheared. These properties are indicative of the presence of a network of long polymer molecules in solution.

The apparent viscosity of the K24 gel sample is dependent on the peptide concentration. For example, a 0.0011 v/v K24 solution in methanol (1.5 mg ml^{-1}) is fluid, whilst a 0.0074 v/v peptide solution (10 mg ml^{-1}) is a solid-like transparent gel. Gels with peptide concentration below 0.02 v/v peptide in methanol are transparent, whilst in more concentrated solutions, particles of insoluble peptide aggregates are dispersed in the gel. In another experiment, a 0.007 v/v K24 rigid gel in methanol was diluted tenfold: after gentle shaking for a few seconds to ensure homogeneity, a fluid solution was obtained. This reversibility of gelation is a characteristic signature of an entangled polymer network. Furthermore, K24 gels in 2-chloroethanol were found to be stable when incubated for 2 h in a thermostatted water bath at various temperatures from 40 to 90 °C (which is close to the boiling point of the solvent). Similarly, the gels of DN1 in water were found to be stable up to the boiling point of water.

Transmission electron microscopy studies

A typical micrograph, obtained with a 0.001 v/v K24 gel in methanol after twentyfold dilution, is shown in Fig. 2(*a*). A network consisting of long polymers randomly distributed on the grid can be seen. Use of a higher peptide concentration results in higher density of polymers on the grid [Fig. 2(*b*)]. In some areas, the polymers form complex entanglements or bundles. In a few cases, they are seen to bend and twist around each other. In areas where their density is lower, individual polymers with straight or wavy edges can be observed.

Regions where individual polymers can clearly be observed were chosen to measure polymer dimensions. More than twenty measurements were made from micrographs of several K24 gel samples. The width was measured to be between 6.6 and 8.1 nm. Overlap of polymers makes it difficult to identify their ends, and to obtain an estimate of their length. Pieces of polymer between points where they meet/cross each other were found to be as long as 120 nm.

K24 does not form a gel in water. Rather, it precipitates out of solution and forms fine, white, solid particles. Such particles were observed with TEM, in order to compare them with the structures in the gel. The micrograph in Fig. 2(*c*) is typical of such a sample. Individual polymers, scattered on the grid are observed. Their width has values between 7.6 and 8.5 nm, and their length is between 38 and 76 nm, *i.e.* they are shorter than the ones in gel forming solvents. Moreover, they do not appear to interact with each other to form bundles or networks as in the case of the gel structure. Rather, a large number of polymers aggregate to form numerous thick amorphous structures.

Characterisation of secondary structure

Infra-red spectroscopy. FTIR spectroscopy was used to probe the conformation of the peptide chains as well as their supramolecular organisation. Peak-fitting analysis of the amide I band of all K24 gel samples studied (which correspond to gels produced in more than 20 different solvents), reveals a single major component centred at 1624.5 ± 0.5 cm^{-1} [Fig. 3(*d*) and (*e*), red spectra] with a half-height bandwidth Dñ equal to 17–19 cm^{-1}. An amide II band centred at *ca.* 1530 cm^{-1} is also observed (not shown). These features are characteristic of a stable homogeneous intermolecular b-sheet structure.[14]

It was estimated from the integrated intensities of the corresponding IR components that *ca.* 90% of the peptide adopts b-sheet structure, such as those obtained in methanol, propanol–D_2O (90 : 10 v/v) and 2-chloroethanol, and the remainder adopts a mixture of random coil and helical conformations, as inferred from the weak components at *ca.* 1645 and 1655 cm^{-1}.

Theoretical as well as experimental evidence has shown that the ratio of the integrated intensities of the weak and strong IR components at *ca.* 1696 and 1625 cm^{-1} respectively, is equal to 0.09–0.19, if the b-sheet consists of 100% antiparallel strands.[14] Peak-fitting analysis of spectra obtained with K24 gels revealed that this ratio is between 0.075 and 0.11, which is indicative of predominantly antiparallel b-sheets. The antiparallel arrangement of peptide strands allows the establishment of stronger interpeptidic hydrogen bonds, leading to the formation of more stable b-sheets than the alternative parallel arrangement.[7] Other factors, such as specific complementary interactions between oppositely charged groups on the N- and C-termini of adjacent peptides, could further contribute to the stabilisation of the antiparallel b-sheet.

Polarised IR spectra of K24 gels spread on a CaF_2 plate showed that the C=O stretching vibration of the peptide backbone at 1625 cm^{-1} is 13% more intense in the direction parallel to the direction of shear as compared to the direction perpendicular to the shear. Assuming that the long axes of the polymers are partially orientated on the direction of shear, this result suggests that the long axis of the peptide b-strand is perpendicular to the long axis of the b-sheet polymer.

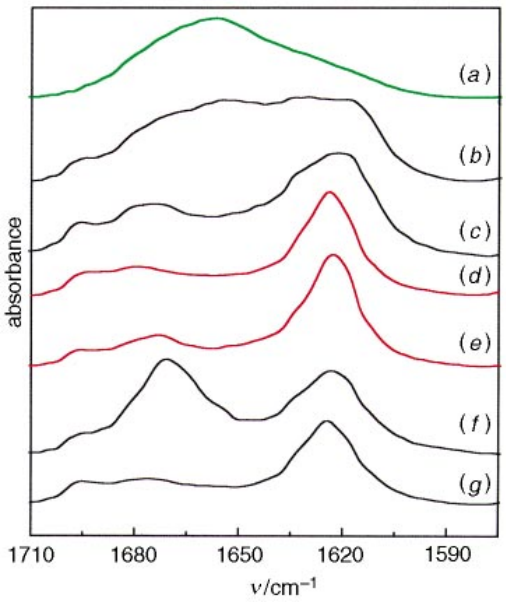

Fig. 3 FTIR amide I bands of 0.004 v/v (2 mM) K24 solutions in: (*a*) HFIP, (*b*) 7 : 3 HFIP–methanol, (*c*) 1 : 1 HFIP–methanol, (*d*) methanol, (*e*) 83 : 17 propanol–D_2O, (*f*) 1 : 4 propanol–D_2O and (*g*) propanol. Colour code: red = gel, green = fluid solution, black = insoluble peptide. The band at *ca.* 1675 cm^{-1} is due to residual TFA, and it is particularly intense in polar solvents.

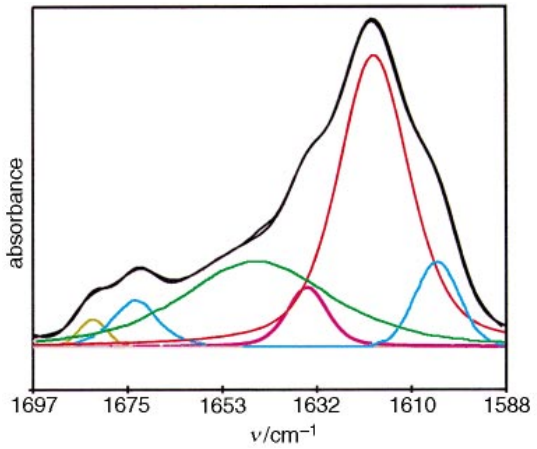

Fig. 4 Peak-fitted FT-IR amide I′ band of 0.003 v/v (5 mg ml^{-1}) DN1 in D_2O. The outer black lines are the experimental and fitted spectra, respectively. Component peaks are shown in different colours. Assignment of component peaks (ref. 35) from right to left: (i) 1604 cm^{-1} = arginine side chain; (ii) 1618.6 cm^{-1} (maximum of amide I′) = b-sheet; (iii) 1633.9 cm^{-1} = glutamine side-chain; (iv) 1645.5 cm^{-1} = residual H_2O; (v) 1673.5 cm^{-1} = residual TFA; (vi) 1683.3 cm^{-1} = antiparallel b-sheet. The half-height width of the major b-sheet component at 1618.5 cm^{-1} is 19.5 cm^{-1}, whilst that of the weak peak indicating antiparallel b-sheet is 10 cm^{-1}.

In the case of DN1, a self-supporting, thermostable gel (up to at least 90 °C) is produced at peptide concentrations above 0.01 v/v (*ca.* 15 mg ml^{-1}) in water. DN1 adopts a b-strand configuration in 0.003 v/v solutions or above in D_2O, as revealed by its IR spectrum (Fig. 4). The major component of the amide I′ band is centred at 1619 cm^{-1} and has half-height bandwidth of 20 cm^{-1}. This main peak is shifted 5 cm^{-1} to lower wavenumbers compared to that on the spectrum of K24, due to the exchange of peptide amide protons by deuterium in the D_2O solvent. A weak peak at *ca.* 1683 cm^{-1} is indicative of a significant amount of antiparallel b-strand arrangements in the b-sheet.

The absence of amide I bands (typically at 1660–1680 cm^{-1}) corresponding to turns for both peptides indicates that they do not adopt a b-hairpin structure but rather a straight b-strand configuration. The simplest arrangement of the peptide, therefore, is an antiparallel arrangement of b-strands aligned perpendicular to the tape long axis, so that they grow in one dimension to form tapes (Scheme 1). The polarised IR results support such an arrangement. Given that the average separation between adjacent residues in a b-strand is 0.335 nm, the length of a 24 residue b-strand is 7.7 nm. This length falls into the range of measured values for the width of the polymers by TEM (6.6–8.1 nm). This observation supports further the presence of tape-like polymers, consisting of extended peptide strands with the strand axis being normal to the polymer's long axis, whilst the direction of hydrogen bonding is parallel to the polymer axis. In this way, K24 peptides could form tape-like structures, whose width corresponds to the length of a K24 b-strand and thickness to that of a single b-sheet (see below).

Self-assembly in dilute solutions

K24. A series of solutions of K24 in methanol were prepared with concentrations ranging from 1–20 mM by taking known amounts of a 2.5 mM stock solution of peptide in HFIP, evaporating to dryness, and dissolution of the resulting peptide film in the required amount of methanol. The far-UV CD spectra are shown in Fig. 5(*a*) as a function of peptide concentration. At peptide concentrations up to 5.2 mM, the spectra exhibit a distinctive isodichroic point at 198 nm indicative of a two-state conformational transition. The variation in intensity of the positive band at 195 nm is indicative of the presence of a strong negative band in the region of 197 nm, characteristic of a disordered conformation. The positive band at 195 nm and the negative band at 216 nm, which increase in intensity with peptide concentration, are indicative of a transition to a b-sheet conformation at higher concentrations. The change in the shape of the spectra at *ca.* 10 mM, but which nonetheless have a minimum at 216 nm, characteristic of a b-sheet structure, is likely to arise from a change in the stacking of aromatic side-chains responsible for the negative band at 203 nm. The plot of the mean residue molar ellipticity in Fig. 5(*b*) is indicative of the progression of the transition with concentration, but due to complexities in the nature of the spectra it is difficult to relate this quantity to the absolute fraction of peptide in the b-sheet state.

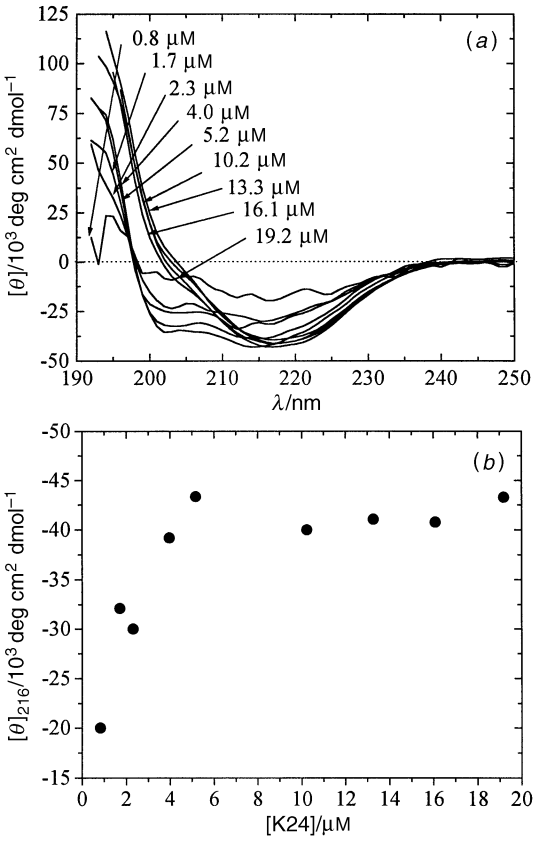

Fig. 5 (*a*) Far-UV circular dichroism spectra of K24 in methanol as a function of peptide concentration: [h] is the mean residue molar ellipticity; (*b*) plot of [h] at 216 nm as a function of peptide concentration

DN1. Similarly, experiments have been carried out on a series of solutions of DN1 in water with concentrations ranging from 10 mM (15.94 mg ml^{-1}) to 450 mM (717.08 mg ml^{-1}) prepared by dilution of a stock solution of known concentration. The stock solution was birefringent after storage for 2 d. Fig. 6(*a*) shows the far-UV CD spectra of DN1 in water as a function of peptide concentration. At peptide concentrations up to 40 mM, the CD spectra exhibit a distinct minimum at 200 nm. This is at a higher wavelength than the value of 197 nm typically found with random coil structures, and is believed to stem from the presence of tryptophan and phenylalanine side chains which absorb strongly in this region.[30] At higher peptide concentrations, a positive band develops in the place of the negative band at 200 nm, and a new minimum develops at *ca.* 224 nm which is attributed to b-sheet structures. Again this peak is at a higher wavelength than the typical value for b-sheet proteins of 217 nm, presumably due to CD

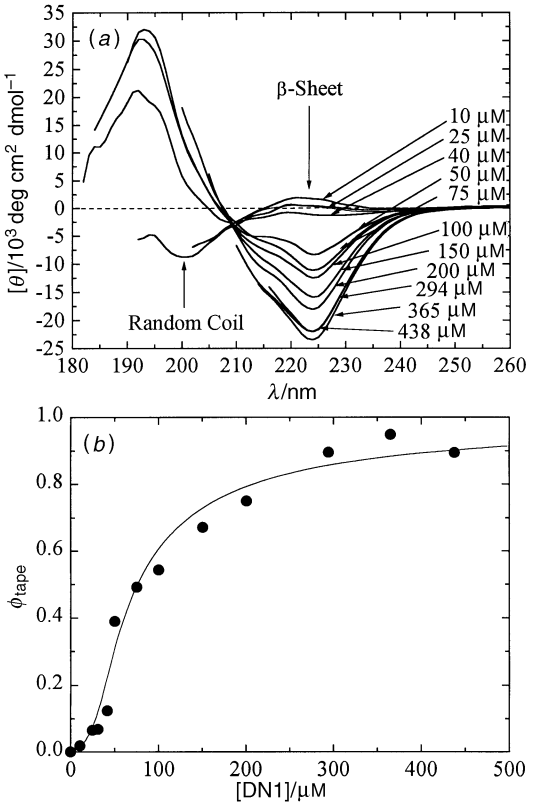

Fig. 6 (*a*) Far-UV circular dichroism spectra of DN1 in H_2O as a function of peptide concentration; (*b*) plot of fraction of peptide in b-sheet states (w_{tape}) as a function of peptide concentration. The continuous line represents the fit of the experimental data to eqns. (5) and (6) using A/n_{link} *ca.* 1.125 mM and E/n_{link} *ca.* 45 mM.

signals from the aromatic side chains in the same region. The isodichroic point at 210 nm is indicative of a simple two state random coil < b-sheet equilibrium. The mean residue molar ellipticity at 224 nm has been taken as a measure of the fractional concentration of peptide in the b-sheet state.

Fig. 6(*b*) shows a slow growth of the fraction of peptide in b-sheet structures up to a concentration of 40 mM, at which it increases suddenly. This behaviour is more complex than expected for a simple one-dimensional association of peptides. In fact, the sudden jump in the fraction of peptide in b-sheet structures is indicative of a critical concentration in the aggregation process, reminiscent of the aggregation of surfactants into sphere-like micelles in aqueous solution. It arises here from the fact that before a peptide monomer can add to a growing tape (see Scheme 1), it must first undergo a transition from, in this case, a random coil to an extended b-strand conformation. The change in free energy involved df (the difference between the free energies of a coil and a b-strand), though significantly smaller than the free energy change, e_{link}, on breaking a peptide–peptide bond in a tape, suppresses aggregation at low peptide concentrations. To demonstrate that this is the case and to obtain values for df and e_{link} we have developed and applied an appropriate theoretical model.

We consider a solution at equilibrium containing tapes having a distribution of sizes such that there are N_m tapes of aggregation number m. If the total number of peptide molecules in a given volume V of solution is N, then eqn. (1) holds.

$$\sum_{i=1}^{2} iN_i = N \qquad (1)$$

The total free energy of the solution is given by eqn. (2),

$$F = N_1(df) + \sum_{m=2}^{2} N_m(m-1)\left(e_{link} - \ln\left[\frac{n_{link}}{n_0}\right]\right) + \sum_{i=1}^{2} N_i \ln\left[\frac{N_i n_0}{V_e}\right] \qquad (2)$$

where df and e_{link} are defined above, n_{link} is the effective volume of a peptide–peptide bond (it characterises how freely a b-strand can move around its neighbour), and n_0 is the intrinsic volume per strand. In order that tapes are stable at some concentration, $e_{link} < df < 0$. The minimisation of the free energy [eqn. (2)] under condition eqn. (1) gives the formulae (3) and (4) for the fractional composition,

$$N_1 \frac{n_{link}}{V} = EL\,, \qquad E \equiv e e_{link} - df \qquad (3)$$

$$N_m \frac{n_{link}}{V} = AL^m, \qquad A \equiv e e_{link} \qquad (m \geqslant 2), \qquad (4)$$

with ln L being the Lagrange multiplier ($0 < L < 1$). The latter can be found using the condition eqn. (1): it is determined indirectly by the total concentration of peptides, eqn. (5).

$$N \frac{n_{link}}{V} = EL + AL^2\left(\frac{2-L}{(1-L)^2}\right) \qquad (5)$$

Finally, the fraction of peptides in tapes (with $m \geqslant 2$), *i.e.* the b-sheet fraction, is given by eqn. (6),

$$w_{tape} \equiv \frac{1}{N}\sum_{m=2}^{2} mN_m = 1 - \left(1 + \frac{A}{E}\frac{L(2-L)}{(1-L)^2}\right)^{-1} \qquad (6)$$

with L being determined by the total concentration as in eqn. (5).

Thus, one can use eqns. (5) and (6) to fit the w_{tape} *versus* peptide concentration data in Fig. 6(*b*) using coefficients A and E as fitting parameters. In doing this we assumed that the measured [h] are a linear function of w_{tape}. Note that the fitted coefficients crucially depend on the value chosen for the link volume n_{link}: A and E being proportional to n_{link}. The best fit which is represented by the continuous line in Fig. 6(*b*) was achieved for: A/n_{link} *ca.* 1.125 mM; E/n_{link} *ca.* 45 mM.

The estimations for the energies entering eqn. (3) and (4) depend on the choice of n_{link}. For $n_{link} = 1$ Å^3, we obtain A *ca.* 6.75×10^{-10} and E *ca.* 2.7×10^{-8}, and hence: e_{link} *ca.* -21.1; $e_{link} - df \# -17.4$; $df \# -3.7$ (in units of k_BT), whilst for $n_{link} = 0.5$ Å^3, we obtain $A \# 8.4 \times 10^{-11}$ and $E \# 3.4 \times 10^{-9}$, therefore:

e_{link} *ca.* -23.2 $\quad e_{link} - df$ *ca.* -19.5 $\quad df$ *ca.* -3.7 (in units of k_BT).

Thus, the values of e_{link} and df are only weakly dependent on the choice of n_{link}. In fact, df is necessarily insensitive to it.

Properties of semi-dilute solutions

Gelation behaviour. The conformational state and gelation properties of both K24 and DN1 peptides have been explored in a variety of solvents. Our observations for K24 are represented in Fig. 7, as a plot of the solvent polarity, e_r, as a function of its hydrogen-bonding ability, a.[15]

Thermostable, self-supporting, mostly transparent gels are found to be stable in solutions of K24 in moderately polar solvents, such as methanol, with e_r in the range 25–68, $a < 1.5$, and peptide concentrations equal to or higher than 0.002–0.004 v/v (region of phase diagram with red dots). For example, 100% propanol ($e_r = 20.1$) produces an insoluble peptide precipitate; mixtures of propanol–D_2O, with volume fraction of D_2O 0.1–0.7 and e_r 26–62, produce gels whose apparent rigidity decreases in mixtures of high volume fraction of D_2O; and mixtures of propanol–D_2O, with volume fraction of D_2O 0.8–1 and e_r 71–80, produce again progressively more insoluble peptide solutions in parallel to increased D_2O content. Studies in methanol–water mixtures as well as in a wide range of other mixed solvents and pure solvents also gave similar results.

In less polar solvents ($15 < e_r < 25$) than the gel-favouring ones, the peptide is not sufficiently soluble to form gels (black

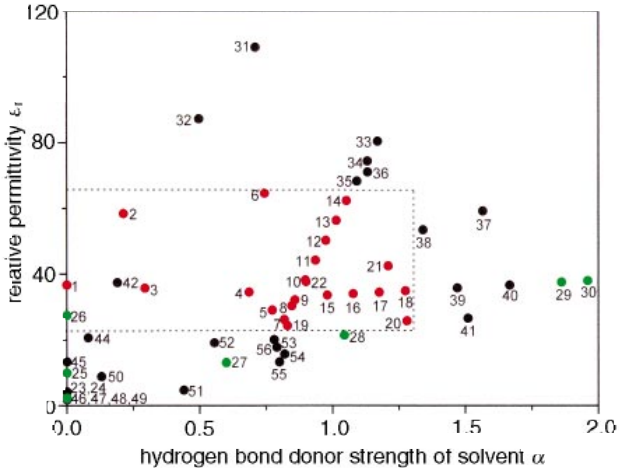

Fig. 7 A correlation plot between the macroscopic properties of 0.004 v/v (2 mM) K24 solutions in various solvents, the relative permittivity e_r of the solvent and its ability to act as hydrogen bond donor, a. The plot was constructed from observations of the IR spectra and mechanical properties of the samples. The dotted lines show the boundaries of the gel region. Each dot represents a solvent with the corresponding e_r and a values. Red = gel, green = transparent fluid solution, black = insoluble peptide. The a and e_r values of mixed solvents were estimated assuming linear relationship between the two component solvents. The number next to each dot refers to a particular solvent: (1) dimethylformamide (DMF), (2) 7:3 DMF–formamide, (3) 7:3 DMF–methanol, (4) 3:7 DMF–methanol, (5) 9:1 propanol–formamide, (6) 1:1 propanol–formamide, (7) 9:1 propanol–water, (8) 83:17 propanol–water, (9) 4:1 propanol–water, (10) 7:3 propanol–water, (11) 3:2 propanol–water, (12) 1:1 propanol–water, (13) 2:3 propanol–water, (14) 3:7 propanol–water, (15) methanol, (16) 9:1 methanol–HFIP, (17) 4:1 methanol–HFIP, (18) 7:3 methanol–HFIP, (19) ethanol, (20) 2-chloroethanol, (21) glycerol, (22) ethylene glycol, (23) benzene, (24) toluene, (25) 1,2-dichlorobenzene, (26) *ortho*-nitrotoluene, (27) benzyl alcohol, (28) 1:1 HFIP–CH_2Cl_2, (29) 1:9 methanol–HFIP, (30) HFIP, (31) formamide, (32) 3:7 DMF–formamide, (33) water, (34) 1:9 propanol–water, (35) 1:4 propanol–water, (36) 1:4 methanol–water, (37) 1:1 HFIP–water, (38) 1:1 TFE–water, (39) 1:1 methanol–HFIP, (40) 3:7 methanol–HFIP, (41) TFE, (42) acetonitrile, (43) acrylonitrile, (44) acetone, (45) THF, (46) diethyl ether, (47) hexane, (48) cyclohexane, (49) cyclohexene, (50) dichloromethane, (51) chloroform, (52) 1:1 methanol–CH_2Cl_2, (53) propanol, (54) 1:1 TFE–CH_2Cl_2, (55) hexanol, (56) butanol.

circles near the bottom of Fig. 7). The fraction of b-structure in these solvents is still as high as in the gel-favouring solvents, *i.e.* equal to *ca.* 0.7–0.9. For example, the peptide which is insoluble in pure propanol ($e_r = 20.1$), has an IR amide I band in this solvent almost identical to the one obtained with its gels [Fig. 3(*g*), estimated percentage of peptide in b-structure: 90%]. A similar situation pertains in solvents with $e_r > 68$ (black circles near the top of Fig. 7). For example, the amide I band in the FTIR spectrum of a peptide solution in 20% v/v propanol–80% v/v D_2O is shown in Fig. 3(*f*). The amide I′ band is centred at 1620 cm^{-1} and the estimated percentage of peptide in b-sheet conformation is equal to 78%.

Consequently, gels are obtained in such solvents which prevent stacking and precipitation of the b-sheets. The average polarity of a K24 molecule, which was estimated to correspond to e_r *ca.* 26, may be a major contributor in determining the optimal solvent polarity required for solvation of tapes and gelation.

In solvents such as 1,1,1,3,3,3-hexafluoroisopropyl alcohol (HFIP) or solvent mixtures with $a \geqslant 1.5$, clear, low-viscosity solutions are obtained (green circles in Fig. 7), even at peptide concentration higher than 0.02 v/v. These simple Newtonian fluid solutions contain peptide molecules in the monomeric state. This is manifested by the absence of b-sheet and the presence of mixtures of helical and random coil peptide conformations, as shown both by FTIR [Fig. 3(*a*): spectrum of peptide solution in HFIP; maximum and half-height bandwidth of principal component of amide I are 1655 cm^{-1} and 30 cm^{-1}, respectively, maximum of amide II at 1545 cm^{-1}], and by CD (minima of negative ellipticity at 208 and 222 nm). A dramatic decrease in the content of the b-sheet is effected by increase of the a-value (and hence of the hydrogen-bond donor strength) of the solvent from methanol to HFIP (Fig. 8).

The peptide is also completely soluble in such solvents as benzyl alcohol, *o*-nitrotoluene, 1,2-dichlorobenzene and benzene (green circles with numbers 27, 26, 25 and 23, respectively, in Fig. 7). The solubilising effect of these solvents is comparable to that of solvents with high a-value. It seems that aromatic groups in the solvent can interact favourably with the six aromatic rings on the peptide and thus compete with peptide–peptide interactions, causing some destabilisation of the b-sheet structure (for example only 60% of the peptide is in b-sheet structure in benzyl alcohol).

Control of the self-assembly process of the b-sheet polymers, as well as of the interactions between polymers, provides ways of tuning the mechanical properties of the peptide gel. One way that the gel-to-fluid transition can be brought about is by varying the hydrogen bond donor strength (a) of the solvent. This can be achieved, for example, in the case of the K24 methanol system quite simply by adding HFIP. The CD spectra in Fig. 9 show the sequential changes in the conformation brought about by 10% increments of HFIP: spectra (i) (10%) to spectra (x) (100%) HFIP. Fig. 9(*a*) shows the conversion from the b-sheet (characteristic minima at 216 nm) to the a-helix (characteristic minima at 208 and 222 nm) conformation [curves (i) to (vii)]. The isodichroic point at 202 nm is confirmation of the simple two state nature of this transition. The accompanying change in secondary structure is illustrated in Fig. 10. Fig. 9(*b*) shows a second isodichroic point associated with a subsequent helix-to-random coil transition [curves (viii), (ix) and (x)].

DN1 shows similar behaviour to K24, apart from the fact that its gel region is shifted upwards towards regions of higher polarity (higher e_r). For example, it produces a self-supporting, thermostable gel, up to at least 90 °C, and at concentrations of 0.009 v/v (*ca.* 5 mg ml^{-1}) or above in water, by self-assembling into b-sheet polymers. In solvents with e_r equal to or less than *ca.* 33, or in the very polar solvent formamide ($e_r = 109$), the peptide is precipitated from solution. Similarly to the behaviour of K24, in solvents with high a-value such as

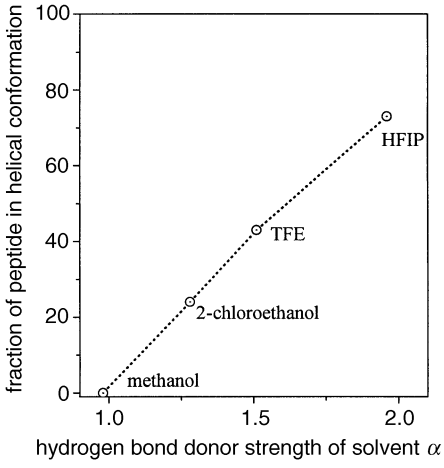

Fig. 8 Plot of the fraction of K24 peptide in helical conformation in *ca.* 0.002 v/v (1 mM) peptide solutions, as a function of the hydrogen bonding strength (a) of the solvent. The fraction of helical conformation was estimated by calculating the ratios of the intensities of the FT-IR peaks at 1655 cm^{-1} (characteristic of helices) and the sum of the intensities at 1655 and 1625 cm^{-1} (characteristic of b-sheet).

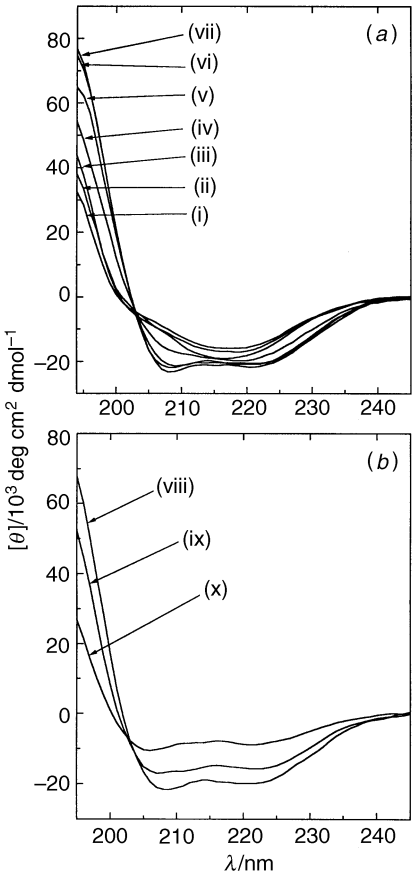

Fig. 9 Circular dichroism spectra of a 27 mM solution of K24 in HFIP–methanol mixtures: (*a*) spectra (i) (10% HFIP) to (vii) (70% HFIP); (*b*) spectra (viii) (80% HFIP) to (x) (100% HFIP)

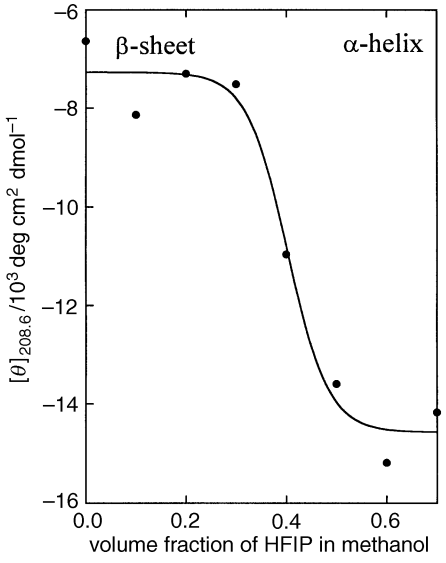

Fig. 10 Relationship between the mean residue molar ellipticity [h] at 208 nm of the CD spectra of K24 solutions in methanol, as a function of the volume fraction of HFIP in these solutions. The more negative the value of the ellipticity, the higher the fraction of peptide in helical conformation. Peptide concentration: *ca.* 0.00006 v/v (*ca.* 81 mg ml^{-1}).

HFIP, the peptide DN1 is fully soluble, and the fraction of peptide in b-sheet is low.

Mechanical properties. To gain further insight into the structure and the dynamics of the gels, we have carried out

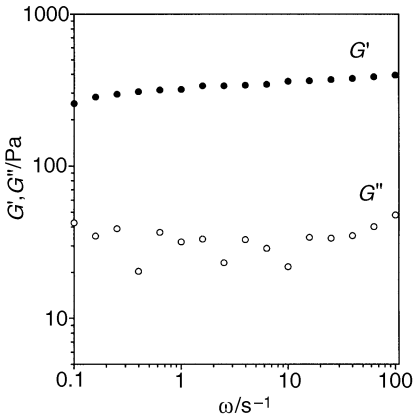

Fig. 11 Typical mechanical spectrum of a 0.02 v/v (9 mM) K24 gel in 2-chloroethanol at 24.8 °C, obtained with small oscillatory shear in the linear viscoelastic region (c = 1%)

rheological measurements on solutions of K24 in methanol and 2-chloroethanol.

A typical mechanical spectrum of a K24 gel in 2-chloroethanol (0.019 volume fraction) is shown in Fig. 11. This was measured using small-strain oscillatory shear experiments (strain: 1–10%). Gels with peptide volume fraction as low as 0.006 were also studied and found to behave in a similar way. The elastic modulus G' is an order of magnitude larger than the viscous modulus G'' indicative of an elastic rather than a viscous material. G' and G'' are seen to be very weakly dependent on frequency v of the oscillatory shear for frequencies 10^{-2}–10^{2} rad s^{-1}, implying that the relaxation time t of the network is very long and not reflected in the measurements. By comparison, for networks of linear synthetic polymers, t is equal to the time t_{rept} required for a polymer strand to reptate out of its entanglement. The longer the polymer, the larger the number of entanglements it participates in, and the longer the network relaxation time. For self-assembling polymers, the relaxation time of the network is equal to the geometric mean of two separate terms, namely the relaxation time t_{rept} due to overcoming entanglements by reptation of the polymers, and the relaxation time t_{break} due to the probability of a self-assembled polymer to break. For example, in the case of worm-like surfactant micelles,[22] G' and G'' cross at *ca.* 1 rad s^{-1}, indicative of much shorter relaxation times compared to the peptide gel network. The long relaxation time of the peptide network is also consistent with the observation that a 0.019 volume fraction K24 gel was resistant to flow for several hours, following inversion of the sample tube. The mechanical spectrum in Fig. 11 supports the presence of stable peptide tapes which are either long and entangled or which form stable chemical crosslinks with each other. Calculations based on the rheological data to be presented below favour the presence of tape entanglements rather than chemical cross-links.

Using rubber-like elasticity theory,[16,17] we have been able to extract information about the mesh size of the peptide network, as well as the persistence length and the thickness of the tapes. The magnitude of $G'_N{}^0$ (plateau elastic modulus) in the linear viscoelastic region (Fig. 11) is related to j, the average distance between two nearest entanglements in space [Fig. 12(*a*)]: eqn. (7),

$$G'_N{}^0 = g_N n_t k_B T \quad (7)$$

where g_N is a numerical factor not far from unity, n_t is the density of network tapes (mol of tapes per cm^3), k_B is the Boltzmann's constant, and T the absolute temperature. j is in effect an upper limit to the mesh size of the network. As there is only one entanglement in volume j^3, thus the density n_e of

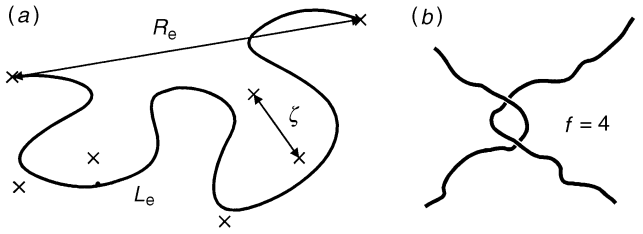

Fig. 12 (*a*) Representation of a network tape, defined as the segment of the random walk tape between nearest crosslink points on the same tape. The crosses are individual entanglement points. For simplicity, no other network strands are shown. (*b*) Entanglement point of a network of polymer chains. Four network chains are involved with it, thus $f=4$.

entanglements is given by eqn. (8)

$$n_e = \frac{1}{j^3} \tag{8}$$

n_e is related to n_t by eqn. (9),

$$n_t = \frac{f}{2} n_e = \frac{f}{2j^3} \tag{9}$$

where f is the number of tapes attributed to each entanglement [Fig. 12(*b*)].

Eqn. (7), (8) and (9) can be combined to yield eqn. (10).

$$j = \left(\frac{g_N f k T}{2 G'_N{}^0}\right)^{1/3} \tag{10}$$

Assuming that f is equal to or greater than 4, and using the magnitudes of $G'_N{}^0$ derived from the mechanical spectra, we estimate the lower limit of j to be in the range (29–43)$\pm$13% nm, for gels with peptide volume fraction in the range of *ca.* 0.019–0.006, *i.e.* the mesh size decreases as the peptide volume fraction increases.

The stress growth *versus* strain curve in Fig. 13 was obtained at a constant shear rate $\dot{c}$ of 100% s^{-1}, with a 0.019 K24 volume fraction gel in 2-chloroethanol. The linear region implies that stress is proportional to strain up to a strain c_{yield} of (230$\pm$45)%. Similar experiments carried out with a 0.006 K24 volume fraction gel gave c_{yield} *ca.* 415% independent of the shear rate $\dot{c}$, 50–100% s^{-1}. These observations as well as the long network relaxation time evident in the mechanical spectra show that there is no significant network relaxation going on during these measurements due to polymer reptation or self-assembly.

At equilibrium, the distance R_e between nearest crosslinks

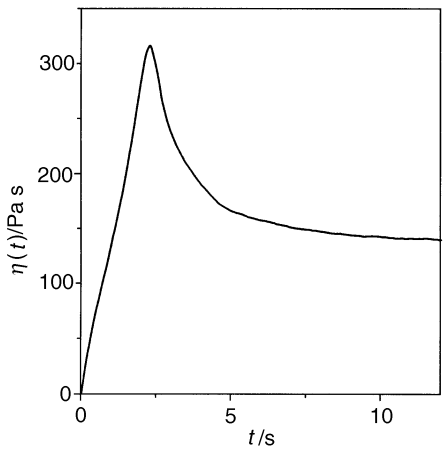

Fig. 13 Stress–strain curve obtained with steady shearing of a 0.02 v/v (9 mM) K24 gel in 2-chloroethanol at 24.8 °C, at constant shear rate $\dot{c}=100\%\ s^{-1}$

on the same tape is equal to or larger than j [Fig. 12(*a*)]. The polymer segment between two nearest crosslinks can be represented as a Kuhn chain consisting of a series of N_e segments each having a persistence length l. As a response to shear, the polymer segments between crosslinks straighten out. The strain at which the tapes are fully extended corresponds to c_{yield}. Further increase in strain causes the tapes to break and the elastic stress to relax. When the applied strain is c_{yield}, then the chain is fully uncoiled and the distance between the same entanglement points is $L_e = N_e l$. By definition, the shear strain c is equal to the ratio of the length under stress and the length at equilibrium, eqn. (11).

$$c_{yield} \# \frac{L_e}{R_e} \# \frac{N_e l}{N_e^{1/2} l} \# N_e^{1/2} \tag{11}$$

N_e was found to be 5.3$\pm$2.0 for a 0.019 volume fraction gel and approximately three times bigger for a 0.006 volume fraction peptide gel. From Fig. 12(*a*), we see that $R_e \geqslant j$. Thus, since $R_e \# N_e^{1/2} l$, we can calculate an upper limit to the persistence length of the tapes using eqn. (12).

$$l \geqslant \frac{j}{N_e^{1/2}} \tag{12}$$

This procedure yields $l \geqslant (12.7 \pm 3)$ nm, indicative of a moderately rigid polymer, consistent with the intrinsic rigidity of b-sheet structures.

Since, the density of network tapes n_t is related to their individual volumes V_t *via* $n_t = w_p / V_t$, where w_p is the volume fraction of polymer in solution and $V_t = L_e\, wt = N_e lwt$, we can get from eqn. (7) an expression of the thickness of a network tape eqn. (13).

$$t = \frac{w_p g_N k T}{G'_N{}^0 N_e l w} \tag{13}$$

Using the following values for a 0.019 K24 volume fraction gel: $w_p = 0.019 \pm 0.001$, $g_N = (1 \pm 0.2)$, $G'_N{}^0 = (328.8 \pm 111)$ Pa, $N_e = 5.3 \pm 2.1$, $l \geqslant (12.7 \pm 3)$ nm, $T = 297.8$ K, and $w = (7.35 \pm 0.70)$ nm, we deduce an upper limit of 0.7 nm for the thickness t of a tape. This value is consistent with tapes a single molecule thick ($0.5 < t_{b\text{-sheet}} \leqslant 1.2$ nm). This result is also in agreement with the notion of an entangled network of tapes.

Discussion

Structure and properties of tapes and networks

The FTIR and CD results for K24 indicate that this peptide adopts an extended b-strand conformation in a pleated b-sheet supramolecular aggregate. The electron micrographs reveal that the aggregates are elongated polymers rather than extended two-dimensional b-sheets. The analysis of the rheological measurements is also consistent with these observations and suggests that the aggregates are nanotapes a single molecule in thickness, *i.e.* thickness equal to 0.5–1 nm depending on the packing of the side-chains (Fig. 14). The estimated length of a 24 residue b-strand is 7.7 nm which falls into the range of the tape width (6.6–8.1 nm) measured by TEM. The rheological measurements have also provided an estimate of a lower limit of 13 nm for the persistence length of the tape, which is indicative of a moderately rigid polymer, consistent with the intrinsic rigidity of b-sheet structures. The tapes in the gels are of the order of microns in length. Whilst an extensive study of DN1 has yet to be made, the IR, CD and gelation studies suggest that it has similar structure and properties to K24.

The initial concentration for gelation is of the order 0.002 volume fraction (1 mM K24). At lower concentrations, the polymer tapes must exist individually. The mesh size of the entangled network in the gels decreases with increasing concen-

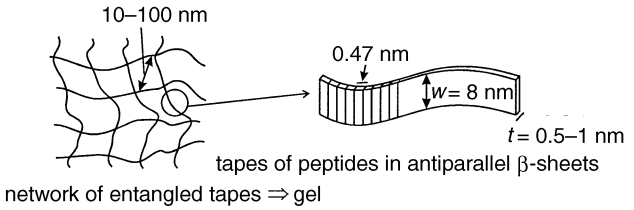

Fig. 14 Schematic representation of an entangled network of K24 b-tapes in a gel, and a single self-assembled peptide nanotape. Each vertical line of the tape represents the long axis of a peptide in a b-strand conformation (length of the b-strand = 7.7 nm). The mesh dimensions of the network correspond to gels with peptide volume fractions from 0.03 to 0.003.

tration: 10–100 nm for K24 gels with volume fraction 0.03–0.003 (Fig. 14).

The thermostability of the tapes is remarkable and presumably stems from the extensive cross-strand side chain–side chain interactions and the extensive network of intermolecular backbone hydrogen bonds. This property, combined with the intrinsic chemical stability of the peptide bond, suggests that these new polymers are quite robust.

Comparison with other biopolymers

The peptide gels (particularly the aqueous ones) in general should be biodegradable and biocompatible. In this respect they can be compared with natural biopolymer gels[18] such as gelatin, actin, amylose and agarose. The elastic (G') and dissipative (G'') moduli of K24 gels are also quite similar with the moduli of most of these biopolymer gels (Table 1).

The mechanical spectrum of the peptide gel in Fig. 11 is flat over the frequency range 10^{-1}–10^{2} rad s^{-1}. Thus G' and G'' are insensitive to the shear rate v, which indicates that the dominant viscoelastic relaxations of the network are at lower frequencies than we have measured (*i.e.* the relaxation time t of the network is long). This is indicative of either very long and stable polymers which are highly entangled, or of strong, non-covalent chemical crosslinks between highly stable polymers. The latter mechanism is responsible for the shear rate insensitivity of G' and G'' of gelatin and agarose gels (Table 1). b-Tape stacking would be an obvious crosslinking mechanism of the peptide polymers. However, the rheology measurements show that the tapes are only one molecule thick, which implies that the best candidates for the crosslink points of the peptide network are topological entanglements of the self-assembled tapes (Fig. 14).

The stress response to strain for a 0.02 v/v peptide gel remains linear up to 230% strain (Fig. 13), which is much higher than for conventional biopolymer gels which typically break at strains of 50% (Table 1). The differences in c_{yield} values indicate that the polymer segments between crosslinks are more flexible (*i.e.* contain more Kuhn segments) in the K24 gel than in the other biopolymer gels. Thus, our peptide gels are less brittle, and stronger than classical biopolymer gels.

The thermal stability of biopolymer gels is shown in Table 1. The peptide gel is more stable at high temperature than most biopolymer gels, apart from alginate polysaccharide gel, which also possesses high thermal stability. This thermal stability of the peptide gels is indicative of a network of strong polymer chains.

We note that other linear biological peptides, such as leucine-rich (LRR) fragments of the drosophila Toll protein,[23] a 28-residue fragment of the b-amyloid protein[24] and peptides modelled on conserved domains of desmin,[25] as well as synthetic peptides incorporating non-natural chemical groups[26–28] have been reported to self-assemble into b-sheet polymers and gel solvents. However, our aim has been to demonstrate the potential for production of b-sheet nanotapes by peptide design.

It is also interesting that the peptide tapes show remarkable similarity in structural terms, to protein fibrils formed *in vitro* and *in vivo* from several different proteins including the polyglutamine-containing proteins responsible for Huntington's disease[29] and the more complex structure of amyloid fibres.[31] For example, amyloid fibrils are rigid, non-branching structures, 10–15 nm in diameter, each consisting of two to five filaments with cross b-structure, arranged in a twisted ribbon pattern. Thus, the peptide tapes may offer a simple model system for studies of the mechanism of fibrillogenesis, which is of crucial importance in many physiological and pathological processes in biology.

Design and self-assembly behaviour

Self-assembly mechanism. The results for the self-assembly behaviour of K24, depicted in Fig. 5(*b*), are of only qualitative significance due to the complexity of the interpretation of the far-UV CD spectra [Fig. 5(*a*)]. However, the behaviour of DN1 whose CD spectra [Fig. 6(*a*)] are interpreted in terms of a simple transition from a random coil to a b-sheet structure are quite similar. They are interesting in that the behaviour is more complex than a simple one-dimensional self-assembly process. This contrasts with the random coil to b-sheet transition of the Alzheimer's b-amyloid fragment which can be described by a simple non-cooperative one-dimensional aggregation model.[32] From Fig. 6(*b*) we see that there is a simple linear association of DN1 up to a concentration of 40 mM, above which there is a sudden increase in the fraction of peptide present in b-sheets, suggesting the requirement of a 'critical tape concentration'. The behaviour is reminiscent of the aggregation of surfactants into spherical micelles in aqueous solution. We have shown that it has its origin in the requirement that before a peptide monomer can add to a growing tape it must first undergo a transition from, in this case, a random coil to an extended b-strand conformation. The change in free energy df for this conversion, though significantly smaller than the free energy change e_{link} on breaking a peptide–peptide

Table 1 Comparison of K24 with other aqueous polymer gels

gel	G'/Pa	G''/Pa	G' plateau/ rad s^{-1}	c_{yield}/%	temperature stability/°C
2.5%w K24 in 2-chloroethanol	330	30	10^{-1}–10^{2}	230	>90
2.2%w gelatin in water	40	—	10^{-2}–10^{2}	<50	⩽35
0.7%w pectin (polysaccharide) in water	100	*ca.* 2	10^{-3}–10		<50
2%w amylose in water	700	200			
1%w agarose (marine polysaccharide) in water	3500	300	10^{-2}–10^{2}	%50	*ca.* 80
Alginate (marine polysaccharide) in water					>100
Carageenan (marine polysaccharide) in water					20–50
2%w xanthane (microbial polysaccharide) in water				%50	
Worm-like micellar aqueous gel	1000		1–10^{2}		
Entangled synthetic polymer network	100				

bond in a b-sheet tape, is quite significant and destabilises small aggregates.

To observe the corresponding transition for K24 will necessitate shifting the 'critical tape concentration' to higher concentrations so as to be detectable by CD spectroscopy. This could be achieved by adding HFIP to the solution. This and other experiments, aimed at controlling the pH and ionic strength of the solution, are in progress.

Peptide Design. The results from our studies of K24 and DN1 suggest a working hypothesis for the design of peptides which will assemble into b-sheet tapes in various solvents, and we are currently involved in a programme of research to rigorously test its validity. The results to date do however establish the viability of engineering nanotapes by peptide design. This opens up opportunities for producing materials with fascinating properties and applications.

The potential to vary the length of a peptide molecule (*i.e.* the tape width), the nature of its side-chains (natural and non-natural), and its environment, provides the means to control the energetics and dynamics of the self-assembly process and consequently, the physical properties of the polymer solutions. There is also the unique opportunity to vary the structure on opposing faces and edges of a tape. In this way tape–tape, tape–surface, and tape–ligand interactions can be controlled. These properties, together with the high temperature stability, biocompatibility and biodegradability make these materials attractive for a wide range of applications.

Prospects for materials chemistry

It is interesting to compare the self-assembly of peptide nanotapes with other studies which have attempted to exploit the intrinsic self assembly behaviour of polypeptides as a route to supramolecular materials. Tirell and co-workers[8] have recently produced novel macromolecular solids by controlling the crystallisation of rationally designed polypeptides. In another study, Ghadiri and co-workers[33] have designed a ring-like peptide molecule, consisting of eight amino acid residues, which self-assembles into long nanotubules. In another study, Zhang and co-workers,[34] have demonstrated that biologically derived linear oligopeptides can self-assemble into extensive b-sheets which condense into macroscopic membranes. Thus, a peptide supramolecular materials chemistry appears to be emerging.

Our work has as its focus the engineering of polymeric b-sheet nanotapes. We believe it should be possible to design and synthesise peptides to generate an entire hierarchy of responsive self-assembled polymer architectures, including homo- and hetero-tapes, dendrimers and cross-linked networks.

This research was supported by the EPSRC, the Wellcome Trust and Schlumberger Cambridge Research. We also thank Dr P. McPhie for assistance with the electron microscopy and Mrs J. L. Johnson for assistance with peptide synthesis.

References

1 J.-M. Lehn, M. Mascal, A. DeCian and J. Fischer, *J. Chem. Soc., Chem. Commun*., 1990, 479.
2 J. A. Zerkowski, C. T. Seto, D. A. Wierda and G. M. Whitesides, *J. Am. Chem. Soc*., 1990, **112**, 9025.
3 J. A. Zerkowski and G. M. Whitesides, *J. Am. Chem. Soc*., 1994, **116**, 4298.
4 K. Hanabusa, T. Miki, Y. Tanaguchi, T. Koyama and H. Shirai, *J. Chem. Soc., Chem. Commun*., 1993, 1382.
5 G. J. Vroege and H. N. W. Lekkerkerker, *Rep. Prog. Phys*., 1992, **55**, 1241.
6 I. A. Nyrkova, A. M. Semenov, J. F. Joanny and A. R. Khokhlov, *J. Phys. II*, 1996, **6**, 1411.
7 T. E. Creighton, *Proteins: Structures and molecular properties*, Freeman, New York, 1993, 2nd edn.
8 M. T. Krejchi, E. D. T. Atkins, A. J. Waddon, M. J. Fournier, T. L. Mason and D. A. Tirell, *Science*, 1994, **265**, 1427.
9 D. G. Osterman and E. T. Kaiser, *J. Cell. Biochem*., 1985, **29**, 57.
10 T. Takumi, H. Ohkubo and S. Nakanishi, *Science*, 1988, **242**, 1042.
11 A. Aggeli, N. Boden, Y. L. Cheng, J. B. C. Findlay, P. F. Knowles, P. Kovatchev and P. J. H. Turnbull, *Biochemistry*, 1996, **35**, 16 213.
12 K. C. Smith and L. Regan, *Science*, 1995, **270**, 980.
13 G. D. Fasman, *Prediction of Protein Structure and the Principles of Protein Conformation*, Plenum Press, New York, 1989.
14 Yu. N. Chirgadze and N. A. Nevskaya, *Biopolymers*, 1976, **15**, 607 and 627.
15 M. J. Kamlet, J. L. M. Abboud, M. H. Abraham and R. W. Taft, *J. Org. Chem*., 1983, **48**, 2877.
16 M. Doi and S. F. Edwards, *The Theory of Polymer Dynamics*, Clarendon Press, Oxford, 1986.
17 J. D. Ferry, *Viscoelastic Properties of Polymers*, Wiley, New York, 1970.
18 A. H. Clark and S. B. Ross-Murphy, *Adv. Polym. Sci*., 1987, **83**, 57.
19 H. McEvoy, S. B. Ross-Murphy and A. H. Clark, *Polymer*, 1985, **26**, 1483.
20 A. H. Clark, M. Watase, K. Nishinari and S. B. Ross-Murphy, *Macromolecules*, 1989, **22**, 346.
21 S. B. Ross-Murphy and K. P. Shatwell, *Biorheology*, 1993, **30**, 217.
22 T. M. Clausen, P. K. Vinson, J. R. Minter, H. T. Davis, Y. Talmon and W. G. Miller, *J. Phys. Chem*., 1992, **96**, 474.
23 D. A. Kirschner, H. Inouye, L. K. Duffy, A. Sinclair, M. Lind and D. J. Selkoe, *Proc. Natl. Acad. Sci. USA*, 1987, **84**, 6953.
24 N. Geisler, T. Heimburg, J. Schuneman and K. Weber, *J. Str. Biol*., 1993, **110**, 205.
25 K. Hanabusa, Y. Naka, T. Koyama and H. Shirai, *J. Chem. Soc., Chem. Commun*., 1994, 2683.
26 H. T. Stock, N. J. Turner and R. McCague, *J. Chem. Soc., Chem. Commun*., 1995, 2063.
27 R. Vegners, I. Shestakova, I. Kalvinsh, R. M. Ezzell and P. A. Janmey, *J. Pept. Sci*., 1995, **1**, 371.
28 A. H. Clark and S. B. Ross-Murphy, *Adv. Polym. Sci*., 1987, **83**, 57.
29 Yu. N. Chirgadze, B. V. Shestopalov and S. Yu. Venyaminov, *Biopolymers*, 1973, **12**, 1337.
30 S. Brahms and J. Brahms, *J. Mol. Biol*., 1980, **138**, 149.
31 C. Blake and L. Serpell, *Structure*, 1996, **4**, 989.
32 E. Terzi, G. Hölzemann and J. Seelig, *Biochemistry*, 1994, **33**, 1345.
33 M. R. Ghadiri, J. R. Granja, R. A. Milligan, D. E. McRee and N. Kzazanovich, *Nature*, 1993, **366**, 324.
34 S. Zhang, T. Holmes, C. Lockshin and A. Rich, *Proc. Natl. Acad. Sci. USA*, 1993, **90**, 3334.
35 W. K. Surewicz and H. H. Mantsch, *Biochem. Biophys. Acta*, 1988, **952**, 115.

Paper 7/01088E; *Received* 17*th February*, 1997